# Chapter 8
# Direct Femtosecond Laser Writing of Nonlinear Photonic Crystals

**Yan Sheng, Xin Chen and Wieslaw Krolikowski**

## 8.1. Quasi-Phase Matching and Nonlinear Photonic Crystals

Nonlinear optical processes, which govern the interaction of strong optical signals (e.g., laser beams or pulses) with the media in which these signals propagate, are of great importance for creation of coherent light sources at the frequency bands where the conventional lasers either perform poorly or are unavailable at all [1]. Moreover, the nonlinear processes are of interest because of their potential application in signal processing, mode-locking, pulse compression, etc. [2-4]. The efficiency of a nonlinear parametric process critically depends on relative phase locking of the interacting waves, which is formally expressed by the so-called phase matching condition requiring that phase velocities of all involved waves coincide. In typical optical media this condition cannot be naturally satisfied due to the refractive index dispersion.

A traditional technique for achieving phase matching in nonlinear crystals is birefringent phase matching, where one exploits angular or/and temperature dependence of birefringence to cancel the phase mismatch [5]. However, this approach is ineffective for weakly birefringent materials and eventually a much more versatile technique, the so-called quasi-phase matching (QPM) which relies on a spatial modulation of the quadratic ($\chi^{(2)}$) nonlinearity, was proposed in the 1960s [6, 7]. This spatial nonlinearity variation offers a set of reciprocal lattice wave vectors to compensate the phase mismatch between the interacting waves. Taking the simplest case of the second harmonic generation in a one-dimensional periodic $\chi^{(2)}$ structure as an example, the QPM condition is written as $k_2$-$2k_1$-$G_m$ = 0, where $k_1$, $k_2$ represent wave vectors of the fundamental and second harmonic beams, respectively, $G_m = 2m\pi/\Lambda$ is the reciprocal lattice vector with $\Lambda$ denoting the period of $\chi^{(2)}$ structure and $m$ being an integer (Fig. 8.1(a)). While initially the QPM structures had been restricted to one-dimensional $\chi^{(2)}$ modulation (also called optical

Yan Sheng
Laser Physics Center, Research School of Physics and Engineering, Australian National University
Canberra, Australia

superlattice), the concept was generalized to two-dimensional structures by V. Berger in 1998 [8]. From then on, the artificial microstructures with a constant linear susceptibility $\chi^{(1)}$, but a spatially modulated nonlinear susceptibility tensor $\chi^{(2)}$ have been called nonlinear photonic crystals (NPC), as a nonlinear optical analogue of the well-known linear photonic crystals [9]. Comparing with the 1D superlattices, the 2D NPC have more plentiful reciprocal lattice vectors in multiple directions, thereby enabling simultaneous phase matching of different nonlinear optical processes in a single crystal (see Figs. 8.1(b) and 8.1(c) for an example) [10]. So far, a variety of NPC structures, including periodic [11], quasi-periodic [12-14], short-range ordered [15,16], radial symmetric [17] and even inherently random nonlinear photonic structures [18, 19], have been developed to facilitate practical applications such as high order harmonic generators [20], optical frequency combs [21], and entangled photon sources, etc. [22, 23].

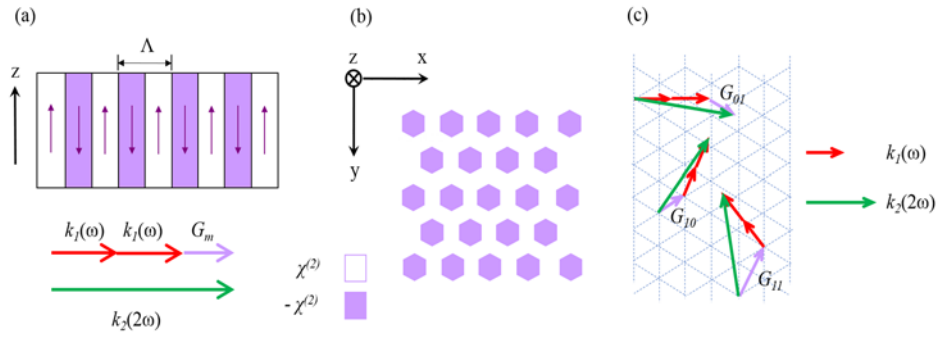


**Fig. 8.1.** (a) Illustrating the concept of quasi-phase matching (QPM) in one-dimensional optical superlattice, where the quadratic ($\chi^{(2)}$) nonlinear coefficient is periodically modulated to compensate phase mismatch of a nonlinear optical process by reciprocal lattice vectors ($G_m = 2m\pi/\Lambda$). (b) An example of two-dimensional nonlinear photonic crystal (NPC), which offers plentiful reciprocal lattice vectors that allow quasi-phase matching of multiple nonlinear optical processes in different directions (c).

## 8.2. Traditional Fabrication Methods of Nonlinear Photonic Crystals

Ferroelectric crystals are the most commonly used materials for the fabrication of nonlinear photonic crystals. In ferroelectrics the area with spontaneous polarization ($P_s$) pointing to the same direction is called a ferroelectric domain. The direction of $P_s$, which actually defines the orientation of ferroelectric domains, can be selectively inverted by applying, e.g. a patterned external electric field so that the second order nonlinear coefficient $\chi^{(2)}$ alters its sign accordingly. The early techniques for ferroelectric domain engineering included stacking thin plates of nonlinear medium where adjacent layers are 180° rotated [24], controlling temperature fluctuation during crystal growth and post-growth engineering of single domain crystals using chemical diffusion and impurities substitution [25]. However, all these techniques have obvious disadvantages and are not suitable for mass production. The situation changed dramatically with introduction of the electric field poling of ferroelectric crystals.

### 8.2.1. Electric Field Poling

In the 1990s the electric field poling (EFP) technique was proposed to achieve periodic ferroelectric domain inversion [26, 27]. It relies on the application of a patterned electric field (higher than the conceive field of the ferroelectric) along the polar direction of the crystal. A typical setup for EFP is illustrated in Fig. 8.2. The electrodes are patterned on the crystal surface (most often by the UV lithography technique), and the spontaneous polarization is reverted only in areas below the patterned electrodes. So far, the EFP has been successfully used to pole various ferroelectrics at a wafer scale, including $LiNbO_3$, $LiTaO_3$, KTP, SBN, etc. It is also widely used to manufacture commercial nonlinear photonic crystals, having capability to pole $LiNbO_3$ crystal as large as 3-inch in diameter [28].

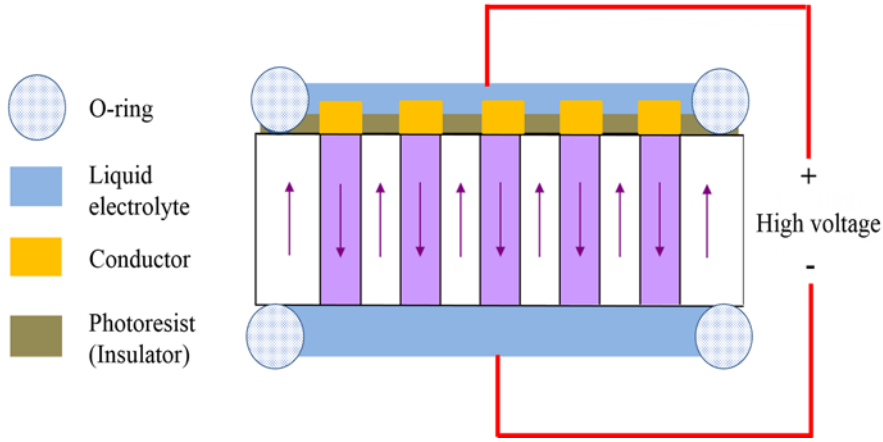


**Fig. 8.2.** A typical setup for electric field poling of ferroelectric crystals. The external electric field is applied to invert ferroelectric domains below the patterned electrodes (conductors). The arrows indicate the spatially varying directions of the spontaneous polarization in the resulting nonlinear photonic crystal.

Although the electric field poling is the most commonly used technique for ferroelectric domain engineering, it suffers from several drawbacks. First of all, the fabrication of ferroelectric domain structures with sub-micrometer accuracy is very challenging. The aspect ratio of inverted domains is usually poor for fine domain periods due to the sideways growth of the reverted domains under electric field [29, 30]. So far only one-dimensional sub-micron periodic domain structures have been reported using this method [31, 32]. Secondly, as the external poling field must be applied along the direction of spontaneous polarization, the method cannot be easily adapted to accommodate samples of atypical (*x*- or *y*-cut $LiNbO_3$) crystallographic orientations. This is a significant disadvantage, since many devices require such atypical crystallographic orientations, for instance, the electro-optic modulators and whispering gallery mode (WGM) harmonic resonators, where *x*-cut $LiNbO_3$ crystal is favoured. Thirdly, it is almost impossible to fabricate three dimensional (3D) domain structures using EFP due to its difficulties in producing *internal* domain inversion. Moreover, the electric poling method is expensive

as it requires specialized poling setups based on photolithographically fabricated electrodes. Any new design or even a minor modification of the QPM structure such as a change of its periodicity requires a new set of structured electrodes.

### 8.2.2. UV Light Poling

The UV light poling was proposed as a method to overcome some of drawbacks of the electric field poling. It involves the use of intense ultraviolet (UV) laser radiations to directly invert ferroelectric domains. The strong absorption of UV light locally heats ferroelectrics to an extraordinary high temperature (typically above the Curie and even melting point), so the coercive field of the crystal is significantly reduced within the optical beam's focal spot [33]. Meanwhile the resulting high temperature gradient leads to the appearance of a thermoelectric field that locally inverts ferroelectric domains when it surpasses the coercive field [34, 35].

Direct UV laser poling eliminates the need of photolithography and high voltage equipment in the traditional electric method. The fabricated domain patterns are directly defined by the position of the laser beam, which offers complete engineering flexibility for precise domain control [37, 38]. The UV method has been used to demonstrate ferroelectric domain patterning with sub-micron periods and arbitrary shapes of individual domains without restrictions of crystallographic orientation [33].

However, the strong absorption of the UV lights is also a cause of serious drawback that limits the practical applications of this technique. The UV-induced ferroelectric domain inversion is usually restricted to a shallow surface layer (usually a few hundred nanometers) [39] and is often accompanied by cracks and surface damages due to the thermal stress during domain formation. As a result, so far no practical devices have been reported based on such UV-inscribed ferroelectric domain structures.

### 8.2.3. Other Poling Techniques

Apart from the electric field poling and UV light poling, there are also a few other techniques for ferroelectric domain engineering. For instance, the light-assisted poling (LAP) uses weakly absorbed laser beam (mainly visible to near IR range, but also some UV wavelengths) to reduce the coercive field of the crystal and a relatively lower homogeneous electric field to reverse ferroelectric domains [40]. The scanning force microscopy (SFM) and electron beam irradiations have also been used to fabricate micro to nanoscale ferroelectric domains, but they are still limited to a very shallow surface layer of the crystal [41, 42].

## 8.3. Direct Femtosecond Infrared Laser Writing of Ferroelectric Domain Patterns

Very recently it has been proposed that the infrared femtosecond laser writing could overcome major drawback of traditional fabrication of nonlinear photonic crystals in

ferroelectrics [43, 44]. The method relies on *nonlinear absorption* of the infrared laser pulses, which induces extraordinary high temperature and steep temperature gradient in the optical beam's focal volume. The coercive field of the crystal may be reduced significantly at such high temperatures and the thermoelectric field induced by the temperature gradient can locally invert the direction of the spontaneous polarization. Since most ferroelectric nonlinear crystals are transparent in the near infrared range, the resulting inverted ferroelectric domains are no longer confined to the surface, but extend deep into the crystal [43]. The nonlinear absorption also allows precise domain engineering with extremely high resolution without optical damage to the crystal surface.

The typical experimental setup for the femtosecond laser direct writing of ferroelectric domain pattern is illustrated in Fig. 8.3 (a).

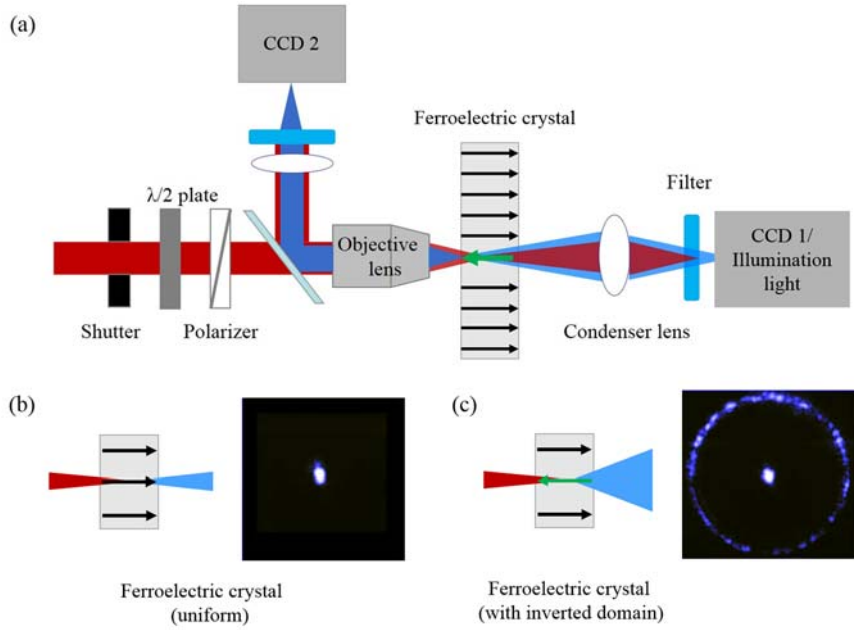


**Fig. 8.3.** (a) Typical experimental setup for the femtosecond laser writing of ferroelectric domain structures. The black arrows inside the crystal represent the initial direction of the spontaneous polarization of the crystal, while the green arrow indicates the reversed polar direction with the ferroelectric domain inversion in optical beam's focal volume. (b) Only a weak collinear (nonphase-matched, forward) SHG is generated in a homogeneous domain crystal. (c) An additional conical Cerenkov harmonic signal is observed when a ferroelectric domain wall is created, which can be used as a real-time monitoring of the infrared light induced domain inversion.

The laser pulses are generated by a femtosecond oscillator (Mira 900, Coherent) operating at 800 nm, with a pulse duration of 180 fs and a repetition rate of 76 MHz. The combination of a half wave plate and a polarizer allows the pulse energy to be adjusted continuously up to 9 nJ. The linearly polarized laser beam is focused by a microscope objective and incident normally to the surface of the sample, e.g. the congruent $LiNbO_3$

crystal, which is mounted on a three-dimensional translational stage. Both the shutter and the translational stage are automatically controlled by computer, thus allowing ferroelectric domain inversion in various patterns.

The setup shown above allows a real time monitoring of domain inversion process by detecting the second harmonic (SH) signal generated by the writing laser pulses. Before domain inversion, only a non-phase matched forward SH propagating collinearly with the fundamental beam (FB) can be recorded by CCD camera 1, as shown in Fig. 8.3 (b). With the laser-induced domain inversion taking place, the so-called Cerenkov SH (CSH) beam appears (Fig. 8.3 (c)), which is a non-collinear SH signal emitted conically at an angle determined by the longitudinal phase matching condition [45]. The is because the Cerenkov second harmonic signal can only be detected when the fundamental beam illuminates a region with spatially modulated $\chi^{(2)}$, for instance a ferroelectric domain wall separating domains with opposite orientations [46]. If the CCD 1 is replaced with a simple illuminating beam, the setup can also be used to monitor the change to morphology of the crystal during the poling process (by CCD 2), including the refractive index changes due to the photorefractive effect.

A critical parameter for laser writing of quality ferroelectric domain patterns is the intensity of the light in the irradiated position, which is mainly related to the incident laser power and the numerical aperture (NA) of the objective. With lower NAs (e.g. 0.2 or 0.3) and full power (about 700 mW), we obtained ferroelectric domain inversion, which, however, had a form of randomly distributed domain islands as revealed by the HF etching. Figs. 8.4 (a-b) show such domain patterns, which are supposed to be two 5 × 5 domain matrices with period of 30 μm. With NA = 0.65 and an incident power of 300 mW, the laser intensity becomes high enough to create inverted domains of regular shapes, as shown in Fig. 8.4 (c). It was also found that domain inversion takes place for beam powers close to a damage threshold above which the laser irradiation would produce ablation spots. Fig. 8.4 (d) shows these spots produced with NA = 0.65 and pulse energy of 5 nJ. The estimated ablation threshold is 0.28 J/cm$^2$. This value is smaller than that reported using single laser shots [47]. Apart from the difference in pulse duration, the main reason is that multiple laser shots result in incubation effects, which consequently lowers the ablation threshold in the crystal [48].

Using microscope objective of NA = 0.65 and pulse energy of 4 nJ, two-dimensional domain patterns with different periods were fabricated. Fig. 8.5 depicts the square lattices with periods of 2 and 1.5 μm, respectively. It is clearly seen that the inverted domains were uniform over the whole area. Almost no domain merging was observed at a 1.5 μm separation between the centers of neighbouring inverted domains, as shown in Fig. 8.5(b). The average diameter of the inverted domains was less than 1.5 μm, which is comparable to the focal spot size of the laser beam. In Fig. 8.6 we apply the infrared laser poling technique to fabricate versatile domain patterns, including square and hexagonal ferroelectric lattices, as well as the decagonal quasi-periodic and short-range ordered domain structures.

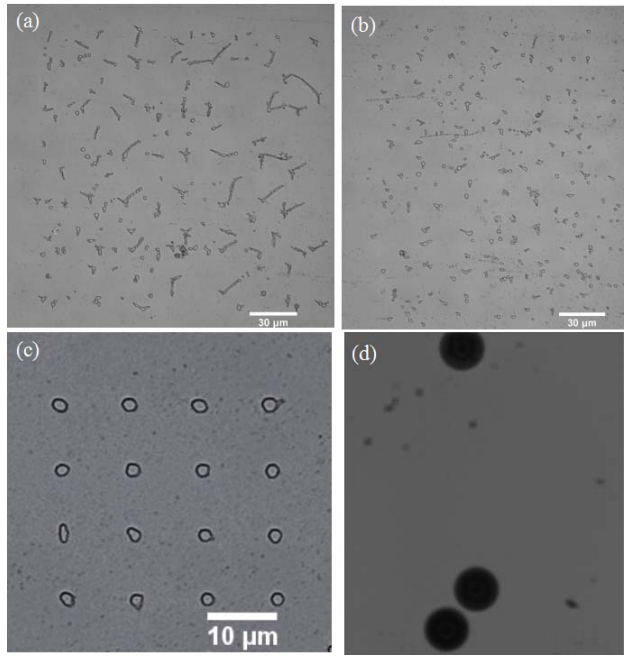


**Fig. 8.4.** Optical microscopic images of the femtosecond-infrared-laser-produced domain patterns after HF acid etching, which are written with (a) NA = 0.2 and pulse energy of 9 nJ, (b) NA = 0.3 and pulse energy of 9 nJ, and (c) NA = 0.65 and pulse energy of 4 nJ, respectively. (d) The optical damage spots produced with NA = 0.65 and pulse energy of 5 nJ.

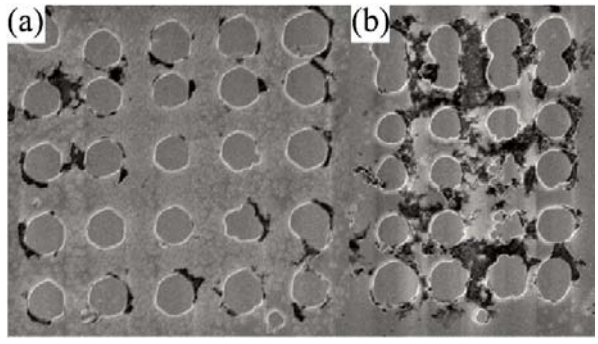


**Fig. 8.5.** Scanning electron microscopy images of the resulting two-dimensional ferroelectric domain patterns in square lattice (after HF etching). The period of the patterns is equal to (a) 2 and (b) 1.5 μm.

The depth and quality of the laser inverted domains were investigated using Cerenkov second harmonic microscopy. Fig. 8.7 shows three-dimensional images of a section of the domain pattern in lithium niobate from Fig. 8.6 (a). It is clearly seen that the femtosecond optical poling method is efficient to produce high-quality domain structures extending over tens of micrometers inside the crystal. In fact, by conducting a series of polishing

and HF etching cycles, the length of inverted domains inside the samples was confirmed to exceed 60 μm.

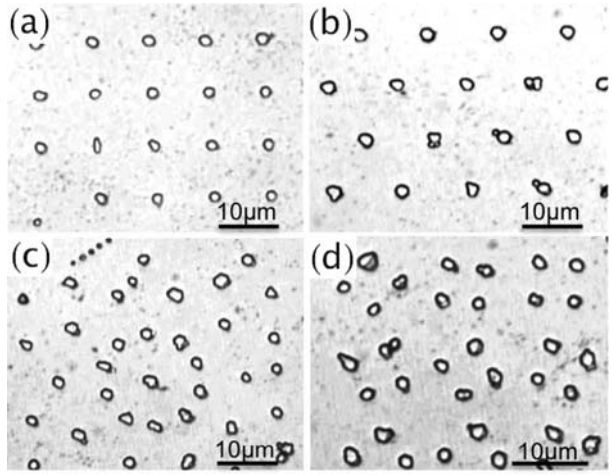


**Fig. 8.6.** Optical microscopic images of two-dimensional ferroelectric domain patterns (after HF etching) formed by femtosecond optical poling. (a) Square lattice; (b) hexagonal lattice; (c) decagonal quasi-periodic; and (d) short-range ordered domain structures.

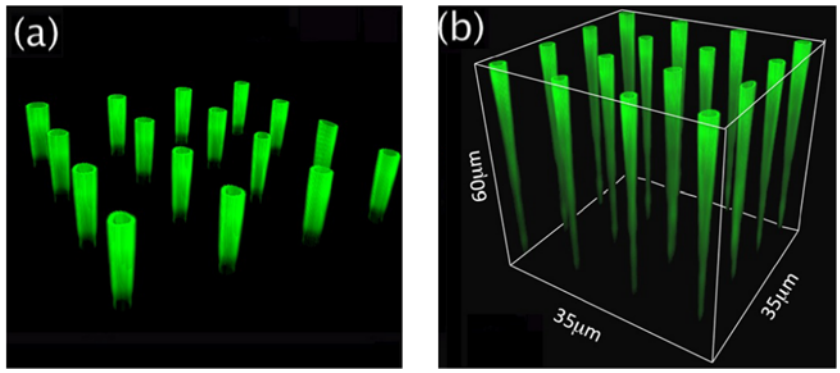


**Fig. 8.7.** Three-dimensional visualization of a section of square pattern of inverted domains by Cerenkov second harmonic microscopy [45, 46]. (a) The first 15 μm deep layer of the pattern (seen from the -z surface) illustrating good quality of the inverted domains. (b) The length of the laser produced reverted domains can exceed 60 μm.

To realize ferroelectric domains inversion deeper inside a crystal, a few factors have to be taken into account. First, the length of inverted domains is affected by the properties of light focusing inside the crystal. It has been well known that high refractive index mismatch between ferroelectrics (like $LiNbO_3$ crystal) and surrounding medium introduces strong spherical aberration, which under focusing conditions, leads to axial deformation of the focal region [49]. Also, when light is tightly focused into a uniaxial crystal along its optical axis, focus splitting occurs [50]. Therefore, measures need to be

undertaken to counteract these effects. For instance, one may use spatial modulation of the incident beam to cancel the spherical aberrations as well as adjust its linear polarization with respective to the crystallographic orientation [51, 52]. Second, the domain reversal could be affected by the temperature-induced stress in the crystal as well as the photorefractive effect. In fact, the refractive index change was observed in the experiment, but it disappeared after annealing the samples at 200 °C for half an hour. The role of these and other factors, such as the focal spot size, heat diffusion, and the ambient temperature, on the quality and efficiency of the domain reversal process needs further investigations.

It is worth mentioning that domain inversion takes place only when the focus of the beam moves along the *z*-axis from the -*z* toward the +*z* surface. In fact, no domain inversion occurred if the beam was tightly focused on the +*z* surface of the sample. These observations indicate the presence of thermoelectric or/and pyroelectric field in the focal volume of the femtosecond beam as a possible cause of domain inversion. In the UV poling this field was induced by a strong absorption of the UV light just below the surface of the crystal. The asymmetry of the thermal profile induces electric field of either thermoelectric or pyroelectric nature, which can locally invert the domain if it is oriented opposite to the direction of spontaneous polarization and its strength exceeds the coercive field. Since the thermal profiles at +*z* and -*z* surfaces are exactly opposite, only the profile near the -*z* surface results in the thermoelectric field oriented against the direction of spontaneous polarization and hence is capable of domain inversion. As lithium niobate is transparent in the infrared, the multi-photon absorption of the high intensity light would heat the crystal in the focal area. While wavelength of the writing laser (800 nm) is too long for band to band two photon absorption (the band gap of lithium niobate is 4 eV), the process could involve two or higher order photon absorption as well as defects or impurity states within the gap [53]. The tight focusing within the crystal ensures a high temperature gradient and, consequently, a high strength of the poling field. In the region where this field exceeds the coercive field, the domain inversion takes place. Moving the focal spot toward the +*z* surface promotes the ferroelectric domain growth along the same direction.

## 8.4. Application of Femtosecond-Laser-Written Domain Patterns in Nonlinear Optics

The infrared laser poling method can be applied in fabricating quasi-phase matching devices, which has been demonstrated in titanium (Ti) diffused $LiNbO_3$ channel waveguides [54]. The waveguide was fabricated by diffusing a 35 nm thick Ti stripe with a width of 3 μm into the -*z* surface of a 500 μm thick congruent $LiNbO_3$ crystal. After a diffusion time of 22 h and a diffusion temperature of 1010 °C, a waveguide with a total length of 10 mm and a width of 3 μm was obtained. The waveguide was designed to be single mode at the pump wavelength of 815 nm, with a refractive index contrast of approximately $\Delta n = 0.001$ and a mode depth of ~ 3 μm. The loss of the waveguide was measured to be around 0.1 dB/cm for both fundamental and second-harmonic TM modes.

A typical optically poled waveguide revealed after HF acid etching is shown in Fig. 8.8(a). The inscribed two-dimensional ferroelectric domain structure covers the whole length of

the waveguide with a period of 2.74 μm in the longitudinal ($x$) direction. In order to cover the whole width of the waveguide, three ferroelectric domains were written in the transverse ($y$) direction with a separation of roughly 1 μm between neighbouring domains. By using Cerenkov second harmonic microscopy to visualize the three-dimensional structure of the optically poled waveguide, as shown in Fig. 8.8(b), the depth of the reverted domains was estimated to be ~28 μm, which ensures a good overlap with the waveguide modes of FB and SH.

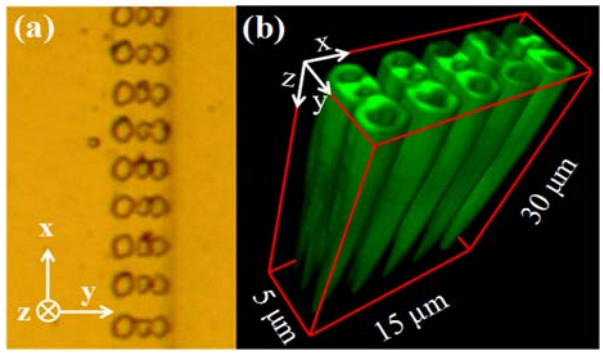


**Fig. 8.8.** (a) Optical microscopic image of the 2-D optically poled $LiNbO_3$ channel waveguide with a period of 2.74 μm in $x$ direction and 1.15 μm in $y$ direction. Individual inverted domains are visible as small circles. (b) Three-dimensional profiles of the inverted domains obtained by the Cerenkov second-harmonic microscopy [45].

The performance of the optically poled waveguide on quasi-phase matched frequency conversion was tested after annealing it at 200 °C for half an hour to remove the remnants of photorefractive effect. The 815 nm fundamental laser beam was generated from a femtosecond oscillator (Mira, Coherent) and focused by a NA = 0.1 microscope objective into the waveguide. The output signals from the waveguide were collected by a NA = 0.1 microscope objective. The powers of the SH were measured after the fundamental beam was blocked by suitable filters. To utilize the strongest nonlinear coefficient $d_{33}$, the fundamental wave was extraordinarily polarized. The waveguide was mounted on a temperature controller to optimize the frequency doubling process. Fig. 8.9 shows the temperature dependence of the SHG efficiency of the optically poled waveguide with a peak efficiency at 62.5 °C. The waveguide exhibited a relatively wide temperature acceptance bandwidth (~5 °C), which is a consequence of a few factors. Firstly, the pulse duration of the fundamental beam in the experiment was 180 fs and the spectral width of such ultrashort pulses is around 15 nm. When the temperature of the waveguide is tuned away from the optimal value at which the central wavelength is quasi-phase matched, the contributions from other spectral components to the SHG grow as they become phase matched. This results in the broadening of the experimental temperature acceptance bandwidth [55, 56]. In addition, the group velocity mismatch between the FB and SH pulses restricted the effective interaction distance of the SHG, which was about 83 μm in the experiment. The shorter the effective length is, the wider the acceptance bandwidth becomes [57, 58]. Another factor responsible for the broadening is the imperfection of the

optically poled domain structures. In any poling processes, the random period errors are unavoidable. Such random deviations from the optimal QPM period will also shorten the effective interaction length of nonlinear processes and broaden the acceptance bandwidth [59].

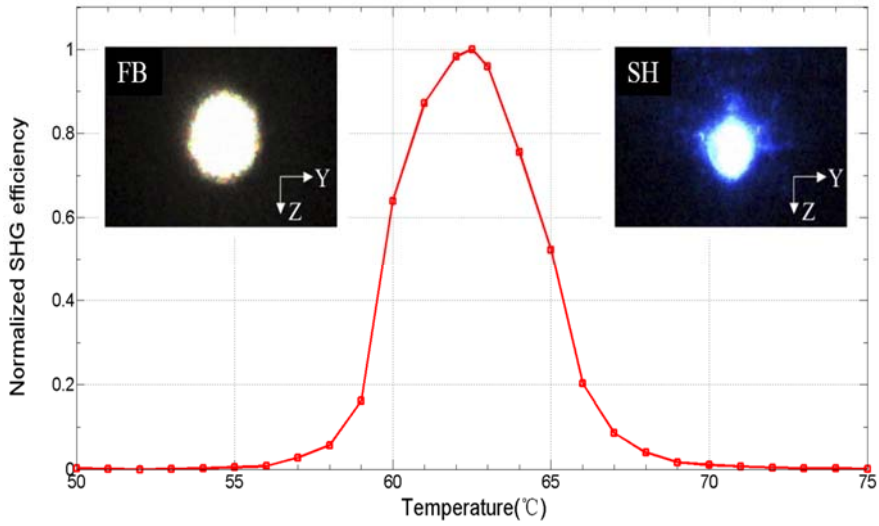


**Fig. 8.9.** Temperature tuning curve of the SHG in an optically poled $LiNbO_3$ waveguide. The insert pictures show the output intensity distribution of the FB and the SH in the far field. The coordinate is that of the $LiNbO_3$ waveguide.

Fig. 8.10 shows the output power and conversion efficiency of the quasi-phase matched SH as a function of the input power of the FB in the laser induced ferroelectric domain pattern. The power of SH follows the square law for low input powers and then the growth slows down above 85 mW in consequence of back conversion. A SH power of 15.3 mW was obtained for 87.6 mW of input power, which corresponds to a conversion efficiency of 17.5 %. Since the experiments were conducted with short pulses, the frequency conversion process was adversely affected by the group velocity mismatch between the FB and SH pulses [55, 56], which restricted the effective interaction length in the frequency doubling process. The SH wave generated within this length can grow coherently. Beyond this length, the newly generated harmonic wave is essentially incoherent with the previously formed, but still contributes to the total output. Therefore, an even higher conversion efficiency can be obtained by using longer (picosecond or nanosecond) pulses and longer samples.

It is worth noting that the femtosecond-laser-inscribed QPM domain patterns basically did not affect transmission characteristics of the waveguide. By comparing the output powers of the FB from the optically poled and pure waveguides in an undepleted pump regime, the average propagation loss caused by the inscribed periodic domain patterns was calculated to be below 0.06 dB/cm, which is two orders of magnitude less than that measured in other femtosecond laser engineered QPM schemes [60, 61].

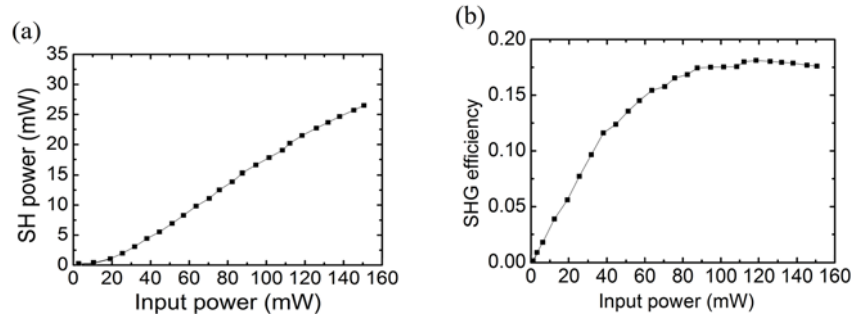


**Fig. 8.10.** (a) Average power and (b) conversion efficiency of the second harmonic versus the average power of the fundamental beam at the optimal QPM temperature 62.5 °C.

## 8.5. Conclusions

We have presented a general review on the commonly used fabrication methods of nonlinear photonic crystals via ferroelectric domain engineering. In particular, we have shown the femtosecond infrared laser direct writing as a promising approach to overcome the insurmountable challenge of other techniques. The infrared laser writing method does not involve any external electric field at any stage of the fabrication process, thereby applicable to ferroelectrics of both typical and atypical crystallographic orientations. Owing to the high transparency of most ferroelectrics in the infrared, the method can also form deep domains inside a crystal, which is a significant result surpassing the capabilities of the optical UV poling technique. The period of the resulting nonlinear photonic crystals can be as small as 1 μm, essential for the productions of fine domain structures. It is expected to achieve even higher resolution by using spatial beam shaping or polarization management. As a demonstration device, we have fabricated a periodic, quasi-phase matching structure in a lithium niobate channel waveguide, and achieved efficient second-harmonic generation at $\lambda = 815$ nm, with 17.5 % conversion efficiency. The femtosecond pulse poling also opens up the possibility to realize true three dimensional domain patterning in the bulk of ferroelectric crystals.

## Acknowledgements

The authors thank the Australian Research Council and Qatar National Research Fund (NPRP 8-246-1-060) for financial support. Xin Chen acknowledges the China Scholarship Council for his Ph.D. Scholarship No. 201306750005. We gratefully acknowledge our collaborators who contributed to the research outcomes presented here.

## References

[1]. R. W. Boyd, Nonlinear Optics, *Academic Press*, 2002.
[2]. G. I. Stegeman, D. J. Hagan, L. Torner, $\chi^{(2)}$ cascading phenomena and their applications to all-optical signal processing, mode-locking, pulse compression and solitons, *Optical and Quantum Electronics,* Vol. 28, Issue 12, 1996, pp. 1691-1740.

[3]. P. H. Pioger, F. Baronio, V. Couderc, A. Barthélémy, C. D. Angelis, Y. Min, V. Quiring, W. Sohler, Spatial routing at 125 Gbit/s based on noncollinear generation of self-trapped beams in Ti:PPLN film waveguides, *IEEE Phot. Techn. Lett.,* Vol. 16, Issue 2, 2004, pp. 560-562.
[4]. M. Bache, O. Bang, W. Krolikowski, J. Moses, F. W. Wise, Limits to compression with cascaded quadratic soliton compressors, *Optics Express*, Vol. 16, Issue 53, 2008, pp. 3273-3287.
[5]. J. E. Midwinter, J. Warner, The effects of phase matching method and of uniaxial crystal symmetry on the polar distribution of second-order non-linear optical polarization, *British Journal of Applied Physics*, Vol. 16, Issue 8, 1965, pp. 1135-1142.
[6]. J. A. Armstrong, N. Bloembergen, J. Ducuing, P. S. Pershan, Interactions between light waves in a nonlinear dielectric, *Physical Review*, Vol. 127, Number 6, 1962, pp. 1918-1939.
[7]. P. A. Franken, A. E. Hill, C. W. Peters, G. Weinreich, Generation of optical harmonics, *Phys. Rev. Lett.,* Vol. **7**, Issue 4, 1961, pp. 118-119.
[8]. V. Berger, Nonlinear photonic crystals, *Physical Review Letters*, Vol. 81, Issue 19, 1998, pp. 4136-4139.
[9]. J. D. Joannopoulos, R. D. Meade, J. N. Winn, Photonic Crystals, Molding the Flow of Light, *Princeton University Press*, 1995.
[10]. A. Arie, N. Voloch, Periodic, quasi-periodic, and random quadratic nonlinear photonic crystals, *Laser & Photonics Reviews*, Vol. 4, Issue 3, 2010, pp. 355-373.
[11]. N. G. R. Broderick, G. W. Ross, H. L. Offerhaus, D. J. Richardson, D. C. Hanna, Hexagonally poled lithium niobate: A two-dimensional nonlinear photonic crystal, *Physical Review Letters*, Vol. 84, Issue 19, 2000, pp. 4345-4348.
[15]. Y. Sheng, J. Dou, B. Ma, B. Cheng, D. Zhang, Broadband efficient second harmonic generation in meida with a short-range order, *Applied Physics Letters*, Vol. 91, Issue 1, 2007, 011101.
[16]. Y. Sheng, S. M. Saltiel, K. Koynov, Cascaded third-harmonic generation in a single short-range-ordered nonlinear photonic crystal, *Optics Letters*, Vol. 34, Issue 5, 2009, pp. 656-658.
[17]. D. Kasimov, A. Arie, E. Winebrand, G. Rosenman, A. Bruner, P. Shaier, D. Eger, Annular symmetry nonlinear frequency converters, *Optics Express*, Vol. 14, Issue 20, 2006, pp. 9371-9376.
[18]. J. Trull, C. Cojocaru, R. Fischer, S. M. Saltiel, K. Staliunas, R. Herrero, R. Vilaseca, D. N. Neshev, W. Krolikowski, Y. S. Kivshar, Second-harmonic parametric scattering in ferroelectric crystals with disordered nonlinear domain structures, *Optics Express*, Vol. 15, Issue 24, 2007, pp. 15868-15877.
[19]. Y. Sheng, X. Chen, T. Lukasiewicz, M. Swirkowicz, K. Koynov, W. Krolikowski, Calcium barium biobate as a functional material for broadband optical frequency conversion, *Optics Letters*, Vol. 39, Issue 6, 2014, pp. 1330-1332.
[20]. W. Wang, V. Roppo, K. Kalinowski, Y. Kong, D. N. Neshev, C. Cojocaru, J. Trull, R. Vilaseca, K. Staliunas, W. Krolikowski, S. M. Saltiel, Y. Kivshar, Third-harmonic generation via broadband cascading in disordered quadratic nonlinear media, *Optics Express*, Vol. 17, Issue 22, 2009, pp. 20117-20123.
[21]. B. Widiyatmoko, K. Imai, M. Kourogi, M. Ohtsu, Second-harmonic generation of an optical frequency comb at 1.55 μm with periodically poled lithium niobate, *Optics Letters*, Vol. 24, 1999, pp. 315-317.
[22]. H. Hübel, D. R. Hamel, A. Fedrizzi, S. Ramelow, K. J. Resch, T. Jennewein, Direct generation of photon triplets using cascaded photon-pair sources, *Nature,* Vol. 466, 2010, pp. 601-603.
[23]. H. Y. Leng, X. Q. Yu, Y. X. Gong, P. Xu, Z. D. Xie, H. Jin, C. Zhang, S. N. Zhu, On-chip steering of entangled photons in nonlinear photonic crystals, *Nature Communications*, Vol. 2, 2011, p. 429.

[24]. M. S. Piltch, C. D. Cantrell, R. C. Sze, Infrared second harmonic generation in nonbirefringent cadmium telluride, *Journal of Applied Physics*, Vol. 47, Issue 8, 1976, pp. 3514-3517.
[25]. E. J. Lim, M. M. Fejer, R. L. Byer, Second-harmonic generation of green light in periodically-poled planar lithium niobate waveguide, *Electronics Letters*, Vol. 25, Issue 3, 1989, pp. 174-175.
[26]. M. Yamada, N. Nada, M. Saitoh, K. Watanabe, First-order quasi-phase matched $LiNbO_3$ waveguide periodically poled by applying an external field for efficient blue second-harmonic generation, *Applied Physics Letters*, Vol. 62, Issue 5, 1993, pp. 435-436.
[27]. H. Ito, C. Takyu, H. Inaba, Fabrication of periodic domain grating in $LiNbO_3$ by electron beam writing for application of nonlinear optical processes, *Electronics Letters*, Vol. 27, Issue 14, 1991, pp. 1221-1222.
[28]. L. E. Myers, Quasi-phasematched optical parametric oscillators in bulk periodically poled lithium niobate, PhD Thesis, *Stanford University*, 1995.
[29]. Y. Sheng, T. Wang, B. Ma, E Qu, B. Cheng, D. Zhang, Anisotropy of domain broadening in periodically poled lithium niobate crystals, *Applied Physics Letters*, Vol. 88, Issue 4, 2006, 041121.
[30]. G. Rosenman, Kh. Garb, A. Skliar, M. Oron, D. Eger, M. Katz, Domain broadening in quasi-phase-matched nonlinear optical devices, *Applied Physics Letters*, Vol. 73, Issue 7, 1998, pp. 865-867.
[31]. C. Canalaia, V. Pasiskevicius, Mirrorless optical parametric oscillator, *Nature Photonics*, Vol. 1, Issue 8, 2007, pp. 459-462.
[32]. M. Shimizu, T. Utsugida, S. Horikawa, K. Fujii, S. Kurimura, H. Nakajima, CW background second harmonic generation with 720 nm-period domains in a QPM adhered-ridge waveguide, in *Proceedings of the Conference on Lasers and Electro-Optics (CLEO'14),* San Jose, California, U.S.A., 8-13 June 2014, p. Stu3H.3.
[33]. C. Y. J. Ying, A. C. Muir, C. E. Valdivia, H. Steigerwald, C. L. Sones, R. W. Eason, E. Soergel, S. Mailis, Light-mediated ferroelectric domain engineering and micro-structuring of lithium niobate crystals, *Laser & Photonics Reviews*, Vol. 6, Issue 4, 2012, pp. 526-548.
[34]. H. Steigerwald, Y. J. Ying, R. W. Eason, K. Buse, S. Mailis, E. Soergel, Direct writing of ferroelectric domains on the *x*- and *y*-faces of lithium niobate using a continuous wave ultraviolet laser, *Applied Physics Letters*, Vol. 98, Issue 6, 2011, 062902.
[35]. A. Boes, T. Crasto, H. Steigerwald, S. Wade, J. Frohnhuas, E. Soergel, A. Mitchell, Direct writing of ferroelectric domains on strontium barium niobate crystals using focused ultraviolet laser light, *Applied Physics Letter*, Vol. 103, Issue 14, 2013, 142904.
[36]. S. Mailis, C. Riziotis, P. G. R. Smith, J. G. Scott, R. W. Eason, Continuous wave ultraviolet radiation induced frustration of etching in lithium niobate single crystals, *Applied Surface Science*, Vol. 206, Issue 1, 2003, pp. 46-52.
[37]. C. E. Valdivia, Light-induced ferroelectric domain engineering in lithium niobate & lithium tantalate, PhD Thesis, *University of Southampton*, Southampton, 2007.
[38]. A. C. Muir, C. L. Sones, S. Mailis, R. W. Eason, T. Jungk, A. Hoffman, E. Soergel, Direct-writing of inverted domains in lithium niobate using a continuous wave ultra violet laser, *Optics Express*, Vol. 16, Issue 4, 2008, pp. 2336-2350.
[39]. A. Boes, H. Steigerwald, T. Crasto, S. A. Wade, T. Limboeck, E. Soergel, A. Mitchell, Tailor-made domain structures on the x- and y-face of lithium niobate crystals, *Applied Physics B*, Vol. 115, Issue 4, 2014, pp. 577-581.
[40]. M. Fujimura, T. Sohmura, T. Suhara, Fabrication of domain-inverted gratings in MgO: $LiNbO_3$ by applying voltage under ultraviolet irradiation through photomask at room temperature, *Electronics Letters*, Vol. 39, Issue 9, 2003, pp. 719-721.
[41]. K. Terabe, M. Nakamura, S. Takekawa, K. Kitamura, Microscale to nanoscale ferroelectric domain and surface engineering of a near-stoichiometric $LiNbO_3$ crystal, *Applied Physics Letters*, Vol. 82, Number 3, 2003, pp. 433-435.

[42]. L. S. Kokhanchik, R. V. Gainutdinov, S. D. Lavrov, T. R. Volk, Characteristics of microdomains and microdomain patterns recorded by electron beam irradiation on Y-cut $LiNbO_3$ crystals, *Journal of Applied Physics*, Vol. 118, Issue 7, 2015, 072001.
[43]. X. Chen, P. Karpinski, V. Shvedov, K. Koynov, B. Wang, J. Trull, C. Cojocaru, W. Krolikowski, Y. Sheng, Ferroelectric domain engineering by focused infrared femtosecond pulses, *Applied Physics Letters*, Vol. 107, Issue 14, 2015, 141102.
[44]. X. Chen, V. Shvedov, P. Karpinski, Y. Sheng, K. Koynov, A. Boes, A. Mitchell, J. Trull, C. Cojocaru, W. Krolikowski, Ferroelectric domain patterning with ultrafast light, *Optics & Photonics News*, Vol. 27, Issue 12, 2016, p. 50.
[45]. Y. Sheng, A. Best, H. Butt, W. Krolikowski, A. Arie, K. Koynov, Three-dimensional ferroelectric domain visualization by Čerenkov-type second harmonic generation, *Optics Express*, Vol. 18, Issue 16, 2010, pp. 16539-16545.
[46]. Y. Sheng, V. Roppo, K. Kalinowski, W. Krolikowski, Role of a localized modulation of $\chi^{(2)}$ in Cerenkov second-harmonic generation in nonlinear bulk medium, *Optics Letters*, Vol. 37, Issue 18, 2012, pp. 3864-3866.
[47]. H. Chen, X. Chen, Y. Zhang, Y. Xia, Ablation induced by single-and multiple-femtosecond laser pulses in lithium niobate, *Laser Physics*, Vol. 17, Issue 12, 2007, pp.1378-1381.
[48]. A. Rosenfeld, M. Lorenz, R. Stoian, D. Ashkenasi, Ultrashort-laser-pulse damage threshold of transparent materials and the role of incubation, *Applied Physics A*, Vol. 69, Supplement 1, 1999, pp. S373-S376.
[49]. M. Gu, Advanced Optical Imaging Theory, *Springer-Verlag*, New York, 1999.
[50]. G. Zhou, A. Jesacher, M. Booth, T. Wilson, A. Rodenas, D. Jaque, M. Gu, Axial birefringence induced focus splitting in lithium niobate, *Optics Express*, Vol. 17, Issue 20, 2009, pp. 17970-17975.
[51]. B. P. Cumming, A. Jesacher, M. J. Booth, T. Wilson, M. Gu, Adaptive aberration compensation for three-dimensional micro-fabrication of photonic crystals in lithium niobate, *Optics Express*, Vol. 19, Issue 10, 2011, pp. 9419-9425.
[52]. P. Karpinski, V. Shvedov, W. Krolikowski, and C. Hnatovsky, Laser-writing inside uniaxially birefringent crystals: fine morphology of ultrashort pulse induced changes in lithium niobite, *Optics Express*, Vol. 24, Issue 7, 2009, pp. 7456-7476.
[53]. S. Juodkazis, M. Sudzius, V. Mizeikis, H. Misawa, E. Gamaly, Y. Liu, O. Louchev, K. Kitamura, Three-dimensional recording by tightly focused femtosecond pulses in $LiNbO_3$, *Applied Physics Letters*, Vol. 89, Issue 6, 2006, 062903.
[54]. X. Chen, P. Karpinski, V. Shvedov, A. Boes, A. Mitchell, W. Krolikowski, Y. Sheng, Quasi-phase matching via femtosecond laser-induced domain inversion in lithium niobate waveguides, *Optics Letters*, Vol. 41, Issue 11, 2016, pp. 2410-2413.
[55]. G. Imeshev, M. A. Arbore, M. M. Fejer, A. Galvanauskas, M. Fermann, D. Harter, Ultrashort-pulse second-harmonic generation with longitudinally nonuniform quasi-phase-matching gratings: pulse compression and shaping, *Journal of the Optical Society of America B*, Vol. 17, Issue 2, 2000, pp. 304-318.
[56]. J. Comly, E. Germire, Second harmonic generation from short pulses, *Applied Physics Letters*, Vol. 12, Issue 1, 1968, pp. 7-9.
[57]. Z. Huang, C. Tu, S. Zhang, Y. Li, F. Lu, Y. Fan, E. Li, Femtosecond second-harmonic generation in periodically poled lithium niobate waveguides written by femtosecond laser pulses, *Optics Letters*, Vol. 35, Issue 6, 2010, pp. 877-879.
[58]. A. M. Weiner, Effect of group velocity mismatch on the measurement of ultrashort optical pulses via second harmonic generation, *IEEE Journal of Quantum Electronics*, Vol. 19, Issue 8, 1983, 1276-1283.
[59]. M. M. Fejer, G. A. Magel, D. H. Jundt, R. L. Byer, Quasi-phase-matched second harmonic generation: tuning and tolerances, *IEEE Journal of Quantum Electronics*, Vol. 28, Issue 11, 1992, pp. 2631-2654.

[60]. J. Thomas, V. Hilbert, R. Geiss, T. Pertsch, A. Tunnermann, S. Nolte, Quasi phase matching in femtosecond pulse volume structured x-cut lithium niobate, *Laser & Photonics Reviews*, Vol. 7, Issue 3, 2013, pp. L17-L20.

[61]. S. Kroesen, K. Tekce, J. Imbrock, C. Denz, Monolithic fabrication of quasi phase-matched waveguides by femtosecond laser structuring the $\chi^{(2)}$ nonlinearity, *Applied Physics Letters*, Vol. 107, Issue 10, 2015, 101109.